Low Open-Circuit Voltage Loss in Solution Processed Small Molecule Organic Solar Cells

Sachetan M. Tuladhar,[*†] *Mohammed Azzouzi,*[†,‡] *Florent Delval,*[†,‡] *Jizhong Yao,*[†] *Anne A. Y. Guilbert,*[†] *Thomas Kirchartz,*[∥,ǂ] *Nuria F. Montcada,*[§] *Rocio Dominguez,*[‼] *Fernando Langa,*[‼] *Emilio Palomares*[§] *and Jenny Nelson*[*†]

[†]Department of Physics and Centre for Plastic Electronics, Imperial College London, South Kensington, London, SW7 2AZ,UK.

[‡] École Polytechnique Universite Paris-Sanclay, 91128 Palaiseau, France

[∥] IEK5-Photovoltaics, Forschungszentrum Jülich, 52425 Jülich, Germany

[ǂ] Faculty of Engineering and CENIDE, University of Duisburg-Essen, Carl-Benz-Straße 199, 47057 Duisburg, Germany

[§]Institute of Chemical Research of Catalonia (ICIQ), Avinguda del Països Catalans 16, 43007 Tarragona, Spain.

[‼] Institute for Nanoscience, Nanotechnology and Molecular Materials (INAMOL), University of Castilla-la Mancha, Campus de la Fabrica, 45071, Toledo, Spain.

AUTHOR INFORMATION

Corresponding Author

* s.tuladhar@imperial.ac.uk ; *jenny.nelson@imperial.ac.uk

ABSTRACT

We analyse the voltage losses at open circuit in solution processed, small molecule: fullerene blend solar cells, using electroluminescence and external quantum efficiency measurements and the reciprocity relationship between light absorption and emission. For solar cells made from oligo-thienylenevinylene based donors and phenyl-C_{71} butyric acid methyl ester ($PC_{71}BM$), we find that the voltage loss due to the finite breadth of the absorption edge is remarkably small, less than 0.01 eV in the best cases, while the voltage loss due to non-radiative recombination reaches 0.29 eV, one of the smallest values reported for an organic solar cell. As a result the open-circuit voltage reaches around 1.0 V for an optical gap of 1.6 eV, greatly exceeding the voltage of a high performance polymer based system with similar optical gap. We assign the remarkably small absorption broadening loss to a low degree of energetic disorder in the small molecule system that allows efficient charge separation at a lower driving force than in typical conjugated polymer blends.

TOC GRAPHICS

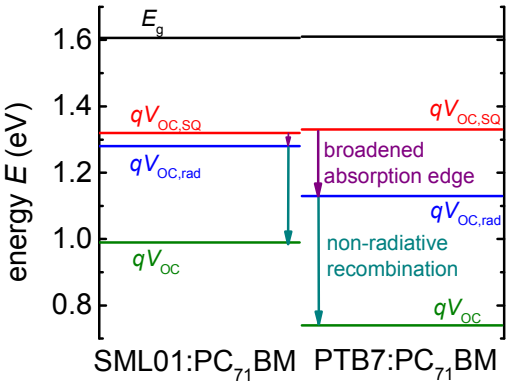

Organic solar cells have attracted intense interest due to the potential for manufacture of solar cells at low cost using solution processing and flexible substrates.[1,2] Research in the field of solution processed organic photovoltaics (OPV) has mostly focused on blends of conjugated polymers with fullerenes due to their high efficiency that has reached 11% in multijunctions[3] and above 10% in single junctions.[4-6] Recently organic solar cells based on low molecular weight solution processed semiconductor molecules (so called "small molecule" organic solar cells) have attracted more attention due to their increasing efficiencies, which have reached record efficiencies of 9-10% in single junction devices[7,8] and 10% in tandem structures[9]. The growing interest in small-molecule optoelectronics is also stimulated by several potential advantages over semiconducting polymers, such as a more reproducible synthesis and the relative ease of purification,[10] whilst maintaining the potential for control of blend microstructure e.g. through use of additives.[11] A further important advantage is the relatively small variation in site energies that may be expected in a small molecule film compared to a conjugated polymer, as a result of the smaller range of backbone conformations available to a small molecule. Such a limited variation in hole or electron energies reduces the so-called energetic disorder of the system; reduced energetic disorder may positively impact the rate of charge transport and the charge

separation yield.[12] Previous studies on high performance small molecule devices indicate that energy losses between the optical gap and the energy equivalent to the open-circuit voltage, eV_{oc}, can be relatively small [13, 14] and that the penalty for charge pair separation may be low[14]. Hence, it is of great interest to analyse and quantify the energy loss processes in small molecule devices in order to understand their potential performance.

We present here a study of the open-circuit voltage (V_{oc}) loss of solar cells based on two different small-molecule donors built around a 3,4-ethylenedioxythiophene (EDOT) group and based on a previously published study of devices made from a family of such materials[15] blended with phenyl-C_{71}-butyric acid methyl ester ($PC_{71}BM$). One of the molecules led to a V_{oc} of 1.0 V, which makes these materials especially interesting for our study of the energy losses in small molecule solar cells. We use methods presented in a recent study[16] to evaluate the different contributions to the loss in V_{oc}. This method uses the concept of a radiative open circuit voltage $V_{oc,rad}$ as previously defined[17, 18] but extends the definition of $V_{oc,rad}$ to respect the actual light absorption spectrum of the solar cell under study. This allows us to assign an upper radiative limit to V_{oc}, $V_{oc,SQ,}$ based on the Shockley-Queisser[19] condition of a sharp absorption edge at the optical gap E_{opt}, and a second limit $V_{oc,rad}$ which replaces the step-function with the measured shape of the absorptance. These assignments allow the losses to absorption edge broadening and non-radiative phenomena to be distinguished.[18,20] In this work we use the external quantum efficiency coupled with electroluminescence spectroscopy to determine the $V_{oc,SQ}$ and the $V_{oc,rad}$ in order to characterise the losses in the open-circuit voltage. The study was extended to different processing conditions, in order to understand the effect of processing-induced changes in film microstructure on the energy loss. The results show that these materials have a very low energy loss compared to polymers with similar optical gap. Moreover, we find that processing

treatments that are known to promote phase segregation also appear to retard non-radiative recombination, as expected. Finally, we attempt to rationalise the low energy loss in these materials using quantum chemical calculations of the excited state spectra of these blend systems.

The small molecules used in our study are 2,2'-((5,5'-((1*E*,1'*E*)-(2,3-dihydrothieno[3,4-*b*][1,4]dioxine-5,7-diyl)bis(ethene-2,1-diyl))bis(3,4-dihexylthiophene-5,2-diyl))bis(methanylylidene))dimalononitrile (SML01) and (5*Z*,5'*Z*)-5,5'-((5,5'-((1*E*,1'*E*)-(2,3-dihydrothieno[3,4-*b*][1,4]dioxine-5,7-diyl)bis(ethene-2,1-diyl))bis(4-hexylthiophene-5,2-diyl))bis(methanylylidene))bis(3-ethyl-2-thioxothiazolidin-4-one) (SML06), both of which are based on a central EDOT moiety, substituted on both sides by thienylenevinylene moiety, and terminated at each end by dicyanovinylene groups (in the case of SML01), or rhodanine groups (for SML06)[15]. Replacing the dicyanovinylene groups with the rhodanine groups lead to a smaller optical gap and higher lying HOMO[15], as confirmed with time-dependent density functional (TD-DFT) calculations (Table S1). The molecules also differ in the number of side chains attached to the thiophenes, which is likely to influence their ability to crystallise. The chemical structures of these small molecules are shown in Scheme 1.

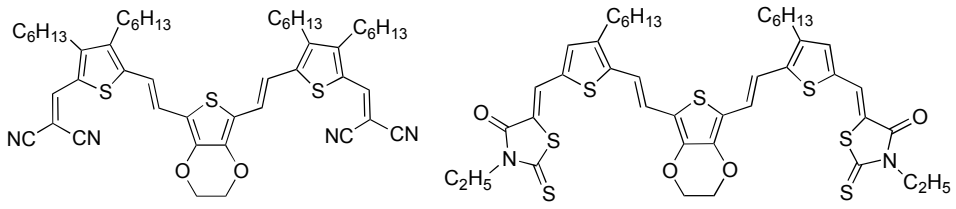

SML01 SML06

Scheme 1. Chemical structures of SML01 and SML06.

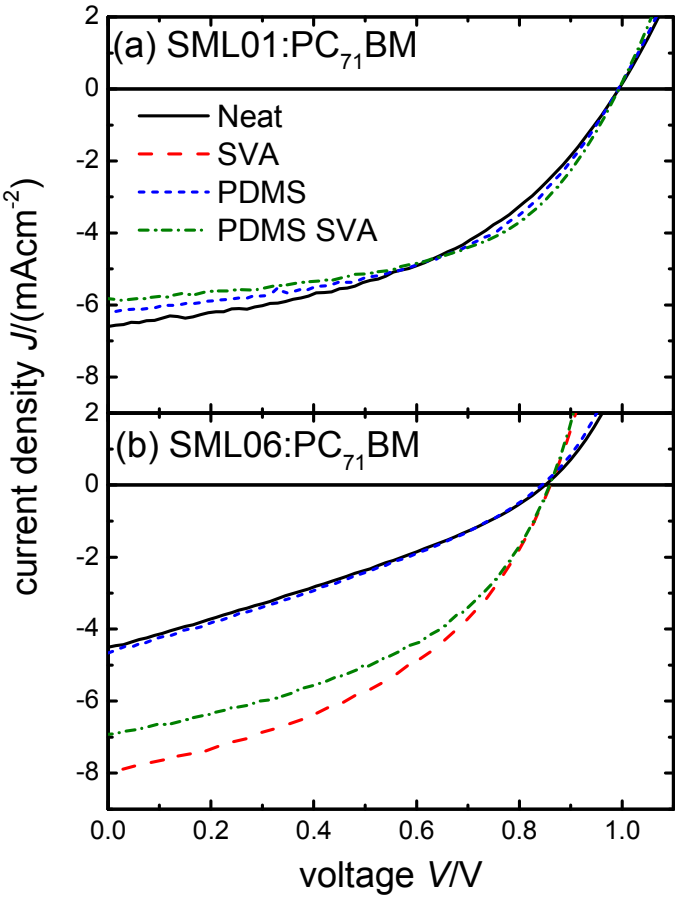

Figure 1. Current vs. voltage (*J-V*) curves under illumination for (a) SML01:$PC_{71}BM$ solar cell devices and (b) SML06: $PC_{71}BM$ solar cell devices that have been processed differently, as follows: 'neat': a blend film with no additive or further processing; 'SVA': neat film that has been solvent vapour annealed in CH_2Cl_2; 'PDMS': a blend film cast from a solution with 0.3 mg/ml PDMS added; 'PDMS SVA': PDMS containing blend that has also been solvent vapour annealed.

Representative current density – voltage (*J-V*) curves obtained from blend devices of the structure glass/ITO/PEDOT:PSS / SML0x:$PC_{71}BM$ (1:1)/Ca/Al are plotted in Figure 1. The results are in good agreement with those in a previous report on these small molecules.[15] In accordance with the HOMO energies and optical gaps of the donor materials, SML06 results in a higher short circuit current density, J_{sc}, whilst SML01 results in a higher V_{oc}. Comparison of different process routes shows that by exposing the film to a solvent vapour annealing (SVA) stage (3 to 5 minutes in CH_2Cl_2 solvent at room temperature) or applying the SVA to a blend film containing 0.3 mg/ml of the inert polymer additive polydimethylsiloxane (PDMS) leads to an improvement of fill factor and consequently power conversion efficiency (PCE). In the case of SML06:$PC_{71}BM$ the effect on J_{sc} is also substantial, as the untreated device suffers from slow charge collection relative to charge generation, which we infer from the poor fill factor. The impact of the processing on V_{oc} is not large in comparison.

To characterise the difference in film microstructure due to processing, we compare atomic force microscope (AFM) images of the film surfaces, before and after solvent vapour annealing, in Figure S1. The SVA treated films appear to show larger domain structures, implying better phase segregation, particularly in the case of SML06. Photoluminescence intensity data (Figure S2) show the effect of SVA more clearly than the surface images. Exposure of blend films to solvent vapour reduces the quenching of the donor PL signal, indicating a growth in the size of pure SML0x domains. In the case of SML06 the domain growth is accompanied by a red shift in the onset of absorption and of EQE (visible on a linear scale in Figure S3) suggesting aggregation of the molecule upon SVA. Crystallisation occurs

readily only in the case of SML06 because of the single alkyl chain on the flanking thiophene in that molecule.

To quantify the losses in open-circuit voltage we have measured the external quantum efficiency (EQE) and electroluminescence (EL) response of the devices. Figure 2 shows the resulting EQE spectra extended to lower energy over several orders in magnitude using the EL data and exploiting the reciprocity relation[21] as done previously.[16,22] Compared to spectra for polymer:$PC_{71}BM$ or evaporated small molecule solar cells,[16, 22-24] the EQE spectra in Figure 2a, and 2b show a remarkably sharp absorption edge over several orders of magnitude for all devices. In addition, it is evident that the EQE for the devices subjected to SVA maintain the sharp gradient over more orders magnitude than the as-fabricated devices for both molecule types.

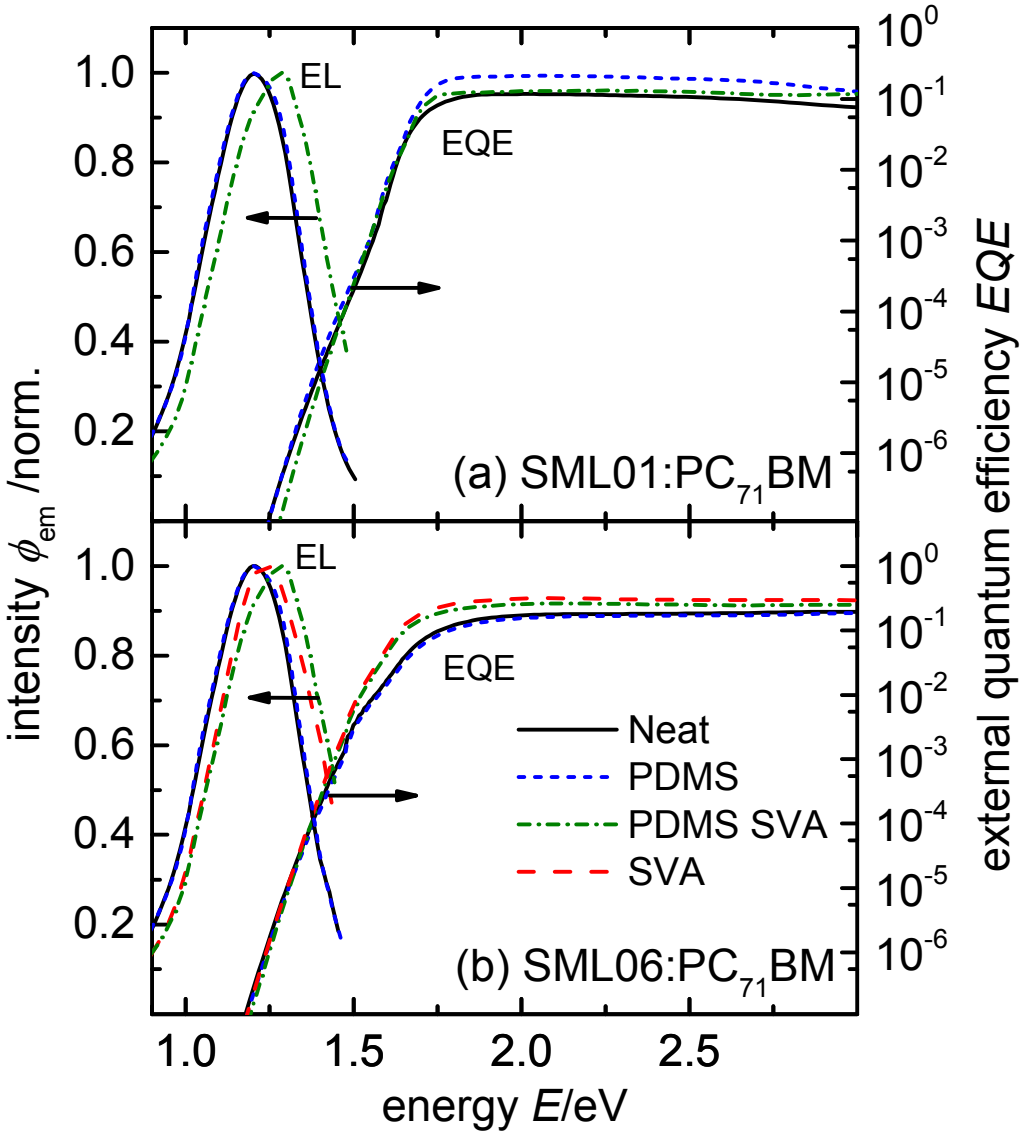

Figure 2. Electroluminescence and external quantum efficiency for (a) SML01:$PC_{71}BM$ and (b) SML06:$PC_{71}BM$ blend device with different processing conditions. The external quantum efficiencies are composed of the directly measured quantum efficiency and the quantum efficiency determined from the EL spectra.

Following previously presented methods[16, 25], we can separate the voltage difference between the optical absorption edge E_{opt}/q where (q is the electric charge) and the measured V_{oc} into three different terms. For an ideal solar cell with a step-function absorptance and perfect carrier collection but in the absence of light concentration or any directionality of light emission, we can define a maximum open-circuit voltage for a material with a given band gap E_g by using the Shockley-Queisser theory. The resulting open-circuit voltage $V_{oc,SQ}$ is typically about 250 mV smaller than E_g/q at one sun illumination. This first component in the energy loss, E_g/q-$V_{oc,SQ}$ cannot easily be associated to any particular loss mechanism but it would be reduced for concentrator solar cells. In the context of organic solar cells this term can be considered as an unavoidable loss mechanism. However, in principle the next two loss mechanisms are avoidable and change substantially from one blend to another.[16] The first of these, $\Delta V_{oc,abs} = V_{oc,SQ} - V_{oc,rad}$, is the loss due to a broadened absorption edge. The so-called radiative open-circuit voltage is, like Shockley-Queisser theory, based on the principle that the only charge carrier loss process is radiative recombination, but it uses the measured absorptance rather than the ideal step-function of Shockley and Queisser to calculate the radiative open-circuit voltage. The more the measured absorptance mimics a step function, the closer $V_{oc,SQ}$ and $V_{oc,rad}$ will be. In contrast large shifts in energy between the main onset of absorption and the tail of absorption, which dominates the luminescence, lead to large values for $\Delta V_{oc,abs} = V_{oc,SQ} - V_{oc,rad}$. In an organic donor-acceptor blend based solar cell this loss can be substantial because the energy of interfacial charge transfer states is often strongly red shifted relative to the onset of strong absorption by the semiconductors. However, if the charge transfer state is barely visible and the luminescence peak is close in energy to the absorption onset, $\Delta V_{oc,abs}$ can in principle also become negative. This is due to the fact that the step-function like absorptance used for the SQ limit always has an

absorptance of 1 at the peak of emission, while the absorptance at the emission peak in the radiative limit can be substantially smaller than one. Thus, the radiative saturation current density can in principle be smaller than the SQ saturation current density without violating the theory. This means that energetic disorder has a small positive effect on V_{oc} and a negative effect on J_{sc}, when compared with a SQ solar cell at a given experimentally determined band gap.

The last loss $\Delta V_{oc,nr} = V_{oc,rad} - V_{oc}$ represents the reduction in open-circuit voltage due to non-radiative recombination. Table 1 summarises the results of this analysis for the devices discussed in the present paper and compares the results to data published in several recent publications that allowed us to perform the same analysis as proposed here.

Table 1. Voltage loss analysis for the small molecule devices and comparison with a range of devices published in the literature and analyzed in the same way. In case of the literature data, we added an abbreviation to show which donor-acceptor combination is used. **P** represents polymer, **F** is fullerene, **SM** is small molecule, '**:**' means donor-acceptor blend and '**/**' indicates a planar heterojunction between a donor and an acceptor. For the devices presented in this paper, the optical gap E_g is determined from the onset of the external quantum efficiency as illustrated in Figure S3.

Blends	E_g	$V_{OC,SQ}$	$V_{OC,rad}$	$\Delta V_{OC,abs}$	V_{OC}	$\Delta V_{OC,nr}$
SML01:$PC_{71}BM$	1.61	1.32	1.28	0.04	0.99	0.29
SML01:$PC_{71}BM$ (PDMS)	1.61	1.32	1.30	0.02	0.99	0.31
SML01:$PC_{71}BM$ (PDMS, SVA)	1.60	1.31	1.31	0.005	0.99	0.32

SML06:$PC_{71}BM$	1.58	1.29	1.21	0.08	0.85	0.36
SML06:$PC_{71}BM$ (PDMS)	1.58	1.29	1.22	0.07	0.85	0.37
SML06:$PC_{71}BM$ (SVA)	1.54	1.26	1.23	0.03	0.88	0.35
SML06:$PC_{71}BM$ (PDMS, SVA)	1.53	1.25	1.24	0.01	0.87	0.37
PTB7:$PC_{71}BM$ [11] (P:F)	1.61	1.33	1.13	0.20	0.74	0.39
PIPCP[a]:$PC_{61}BM$ [14] (P:F)	1.41	1.15	1.16	-0.01	0.89	0.27
DBP:ZCl[b] [26] (SM:SM)	1.95	1.66	1.58	0.08	1.33	0.25
DTD:N2200[c] [27] (SM:P)	1.55	1.27	1.16	0.11	0.82	0.34
PTB7-Th:IDTIDT-IC[d] [28] (P:SM)	1.53	1.25	1.28	-0.03	0.94	0.34

[a]PIPCP contains a backbone comprised of CPDT-PT-IDT-PT repeat units (CPDT = cyclopentadithiophene, PT = pyridyl[2,1,3]thiadiazole, IDT = indacenodithiophene);
[b](tetraphenyldibenzoperyflanthrene : zinc chlorodipyrrin);
[c] (diketopyrrolopyrrole-thieno[2,3-f]benzofuran : commercial polymer acceptor);
[d] (poly(thieno[3,4-b]thiophene/benzodithiophene) : indacenodithiophenoindacenodithiophene)

Both optical gap and V_{oc} are larger for SML01 than SML06. In the case of SML06 only, the band gap is reduced by up to 0.05 eV upon SVA. This is due to the greater ability of this molecule to crystallise upon annealing, also suggested by the domain growth in Figure S1and S2. In all $V_{oc,SQ}$ lies 0.28 – 0.29 V below the optical gap. The loss in actual V_{oc} compared to this maximum, i.e. $\Delta V_{oc,abs} + \Delta V_{oc,nr}$, varies between 0.32 and 0.44 V. Compared to many typical polymer:fullerene solar cells[11] the avoidable loss $\Delta V_{oc,abs}$ due to the non-sharp absorption edge is very small, between 0.01 and 0.08 eV compared, for example, to 0.20 eV in the case of PTB7:$PC_{71}BM$.

The non-radiative voltage loss $\Delta V_{oc,nr}$ of these materials ranges from 0.29 to 0.37 V and in the best cases is lower than the lowest previously published values for polymer:fullerene solar cells which were 0.32 V for an indacenodithiophene polymer[29] and 0.34 V for a diketopyrrolopyrole based polymer[16]. However, even lower values can be found in the literature if the present analysis is applied to published data. The lowest values for $\Delta V_{oc,nr}$ that we could

find were 250 mV for an evaporated bilayer solar cell reported in Ref [26] and 270 mV for a polymer:fullerene bulk heterojunction solar cell reported in Ref [14]. Other relatively low values that have been published recently are 340 mV for both a small molecule:polymer blend and a polymer:small molecule blend both of which have no fullerene acceptor.[27,28] Thus, low voltage losses can be found for all combinations of donor and acceptor molecules. However, it can be noted that material combinations including either a small molecule donor or a non-fullerene acceptor are very well represented among the materials with very low voltage losses. In the following we consider possible reasons for low voltage losses in the blends based on thje small molecules SML01 and SML06.

The combination of low $\Delta V_{oc,abs}$ and $\Delta V_{oc,nr}$ explains the high open-circuit voltages that we could achieve with these materials. Whilst the origin of the relatively low non-radiative loss is not known, it is consistent with the higher degree of purification possible for small molecules than for polymers, which could reduce the defect density, and also with the lower degree of disorder in electronic state energies that is expected in small molecules due to their limited conformational phase space . In the case of the SML06 devices, the non-radiative loss is lower after SVA. This is consistent with the longer charge recombination time observed for the SVA relative to the non-annealed devices using transient-photovoltage measurements (Figure S4). As established previously[15] SVA appears to lead to larger domains and therefore less interfacial area. It has been shown elsewhere that reduction in interfacial area in bulk heterojunctions can improve V_{oc} by reducing non-radiative recombination losses[24] and it is consistent with the fact that the lowest $\Delta V_{oc,nr}$ we found was for a bilayer system where the interfacial area is naturally minimized.

We notice as well that the solvent vapour annealing stage decreases $\Delta V_{oc,abs}$ for SML06 samples by at least 0.03eV. This is due to the sharpening of the absorption edge that is observed upon SVA, which was assigned to aggregation of SML06.

Compared to most polymer:fullerene systems (see e.g. Ref [16]), the SM devices show exceptionally low absorption broadening losses and a V_{oc} that is closer to the optical gap. In order to understand why these small-molecule devices show a low voltage loss, especially the one due to the absorption edge, we have used time-dependent density functional theory (TD-DFT) to investigate the electronically excited states of the donor : acceptor complex for different positions of the fullerene ($PC_{71}BM$) relative to the donor molecule.[30,31] We calculated the excited states and their electronic density distribution using TD-DFT with B3LYP/6-31G* in vacuo with Gaussian 09[32]. Whilst we recognize that the B3LYP functional has known limitations that affect the study of charge transfer (CT) CT states, we selected this functional because it has shown good agreement with experimental trends in CT state energy with changes in chemical structure[30] and it has been shown to reproduce experimental data as well as more expensive methods[33]. For the present study we first confirmed that the method reproduced the relative HOMO energies and optical gap of the two small molecules correctly. The results of the calculation for different position of the fullerene (on top of the central EDOT, the flanking thiophene (labelled T1), or the terminal group (labelled Rhod or CN)) are shown in Figure 3. These positions are presented in Figure S5. The different states are classified as being CT states, when most of an electronic charge is transferred to the fullerene, excitonic, when the excitation is localized largely on either donor or acceptor, or mixed in the intermediate case.

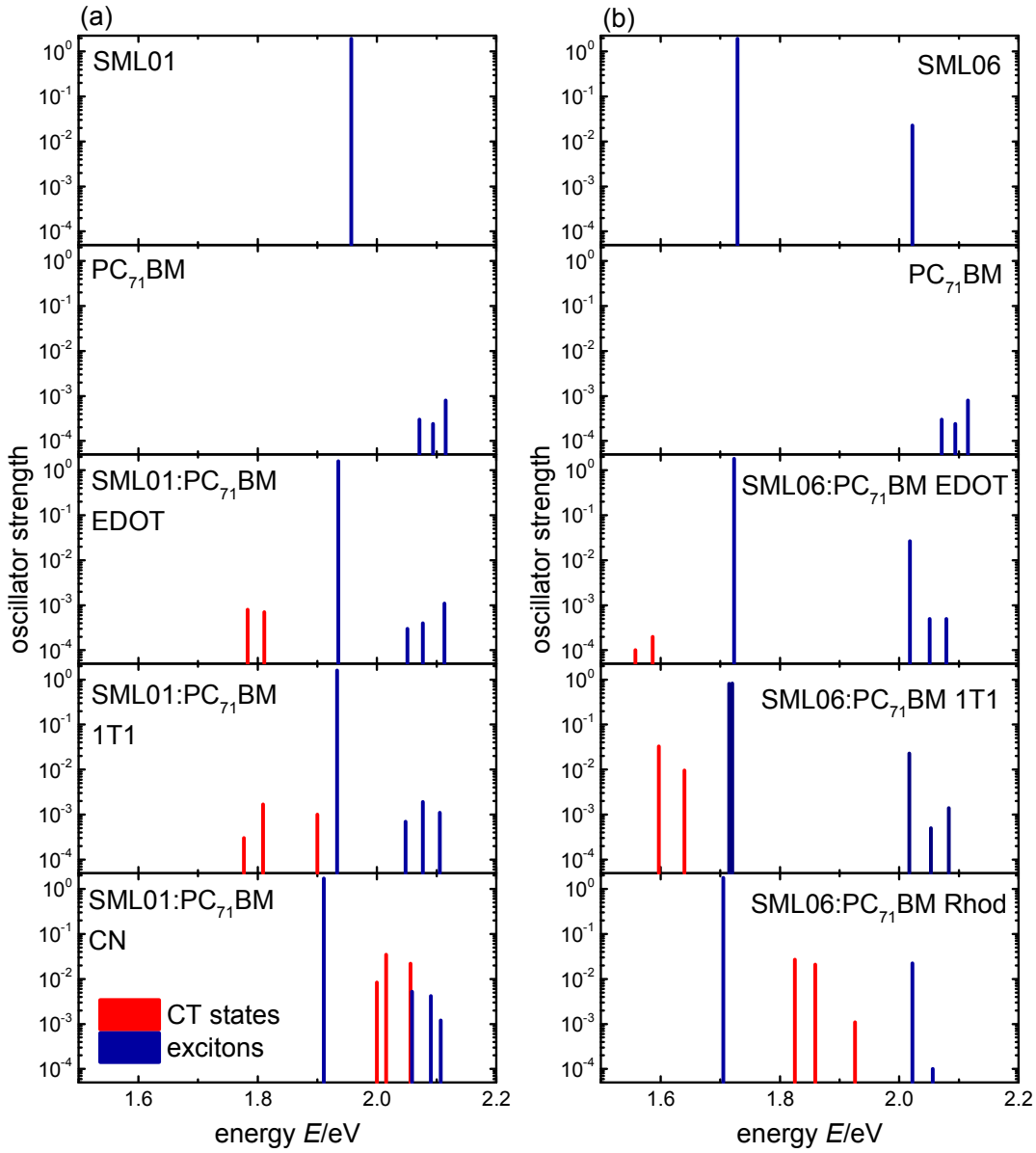

Figure 3. TD-DFT calculation of excited states of SML01, SML06 and for SML01:$PC_{71}BM$ and SML06:$PC_{71}BM$ complexes with the $PC_{71}BM$ in three different positions relative to the donor molecule.

When the fullerene is placed above the acceptor (Rhod or CN) part of the molecules, there is no charge-transfer state at an energy below the exciton state. For both the T1 and EDOT positions, the lowest state is a charge-transfer state, and although the charge-transfer state for the EDOT position lies lower in energy, the energies of the CT states for the different positions lie within some kT (0.025eV) of each other. From these calculations we will consider the CT state to be the first excited state for the complex where the fullerene is in the EDOT position, i.e. the lowest excited state of all geometries considered. We hence obtain a (value for the exciton – CT state energy difference) of 0.15 eV. The relatively small difference between the CT state and donor exciton energy could explain the low voltage loss observed for these materials. In fact, we can compute the absorption from the oscillator strength (Figure S6); these plots confirm that a sharp, approximately exponential absorption edge is expected for these calculated transitions and that the sharp edge is compatible with the low $\Delta V_{oc,abs}$ observed.

In polymer based systems, current generation is observed to depend on the interfacial driving force, and typically switches off when that the exciton-CT state energy gap drops below ~0.3 eV[34]. There are exceptions where efficient generation occurs at lower driving force, for example in an isoindigo polymer[35,36] and a diketopyrrolopyrrole terthiophene (DPP3T) polymer[37] as well as for the four systems listed at the bottom of Table 1. For DPP3T:PCBM, for instance, $\Delta V_{oc,abs}$ = 0.02 eV[16] while the calculated exciton-CT state energy difference using a DPP3T oligomer: PCBM complex is 0.15 eV, using the same methods as used for the SML0x:PCBM complexes here (Figure S7) This value of 0.15eV is similar to the small molecule systems studied here and smaller than the calculated exciton-CT state difference for the majority of polymer:fullerene combinations used in solar cells[27] (calculated using the same level of theory).

Thus, relative to typical polymer:fullerene systems, the SML01 and SML06 systems show charge separation at unusually low exciton-CT state energy gaps. The larger threshold for charge separation usually seen in polymer systems may result from a larger degree of conformational disorder in the polymer compared to small molecules, leading to disorder in the CT state energies and correspondingly inefficient separation for the fraction of CT states lying in the low energy tail. For the small molecule systems we expect less disorder in both exciton and CT energy as a result of the reduced number of donor: acceptor configurations, relative to a polymer: fullerene system. We explored the effect of conformational disorder in the small molecule on exciton and CT state energies and found that distortions of the small molecule backbone conformation that are expected at room temperature affect the position of CT and exciton by < 20 meV and cause a relatively minor broadening of the absorption spectrum (Figure S8). We propose that the efficient charge separation at low driving force in small molecule based systems results, at least in part, from the relatively low energetic disorder in the system, and that this is what enables the relatively sharp EQE edge of the small molecule fullerene system, and hence the low losses in V_{oc}.

In conclusion, we have investigated the voltage loss in a small molecule solar cell using a quantitative analysis of the loss processes based on quantum efficiency and electroluminescence measurements. We have found that for SML01 and SML06, the absorption edge is very sharp thereby considerably reducing the associated losses in open-circuit voltage. Additional processing steps such as solvent vapour annealing lead to a further reduction in voltage losses, probably due to phase segregation and a reduction in interfacial area. Time-dependent DFT calculations on the donor-acceptor interface show that the energy difference between the lowest charge-transfer state of the donor-acceptor complex and the donor exciton is around 0.15 eV and

lower than the threshold for efficient charge generation in typical polymer based systems. We suggest that the high charge generation efficiency at low energetic driving force results from reduced disorder in the electronic energies of small-molecule, compared to polymer, systems.

Experimental Methods

The devices were fabricated with the layer structure glass/ITO/PEDOT:PSS/SML0x:$PC_{71}BM$/Ca/Al. The substrates were cleaned by ultrasonic treatment in acetone, and isopropyl alcohol and subsequently blow-dried with nitrogen. The surfaces of the ITO substrates were processed in ozone at 100 W for 5 minutes. Subsequently, a hole transport layer PEDOT:PSS (Clevios PVP AI 4083, filtered at 0.45 μm) was deposited by spin-coating at 3500 rpm (thickness around ~30 nm) onto the ITO surface and then annealed at 150 °C for 20 min. The organic films were deposited from a solution containing SML0x and $PC_{71}BM$ in a weight ratio of 1:1 at a solid concentration of 20 mg/ml in chloroform. Another solution was prepared with the same condition but also containing 0.3 mg/ml of PDMS (molecular weight 14000 g/mol).

The active layer was spin-coated at 8000 rpm with acceleration 4000 rpm/s, yielding a thickness around 75 nm. Where necessary an additional step was also carried out straight after deposition of the active layer by exposing the films to a saturated vapour of dichloromethane solvent (CH_2Cl_2) in a sealed closed vessel (solvent vapour annealing, SVA). The films were exposed to the solvent vapour for 3-5 minutes. Finally, the layers of the top electrode, Ca (~20nm) and Al (~100 nm), were deposited subsequently at a rate of 0.1Å/s through a shadow mask with an aperture area of 0.045 cm^2 under a constant pressure less than 10^{-6} Torr. Current

density–voltage (J–V) characteristics of the devices were measured using a Keithley 236 Source Measure Unit and a xenon lamp with AM1.5G filters and 100 mW/cm² illumination solar simulator (Oriel Instruments).

Electroluminescence (EL) was measured using a Shamrock 303 spectrograph combined with an iDUS InGaAs array detector cooled to –90 °C. The driving injection current is in the range of 1.25 and 1250 mA/cm^2. The obtained EL spectra intensity was calibrated with the spectrum from a calibrated halogen lamp.

External quantum efficiency (EQE) was measured using a grating spectrometer (CVI DIGIKROM 240) to create monochromatic light combined with a tungsten halogen light source. The monochromatic light was chopped at 235 Hz and Stanford Research Systems SR380 lock-in amplifier with an internal transimpedance amplifier of 10^6 V/A was used to detect the photocurrent. Long pass filters at 610, 715, 780, 850, and 1000 nm were used to filter out the scattered light from monochromator. The spectra were taken from 350 to 1100 nm and calibrated by a silicon photodiode.

PL Steady-state: PL was collected using a Horiba Jobin Yvon Fluorolog-2 PL spectrometer.

TD-DFT: Ground state energies and geometries were calculated using Density Functional Theory (DFT) with B3LYP functional and 6-31G* basis set in Gaussian 09[29].We estimate the LUMO levels from the first excited state of a time-dependent DFT (TDDFT) calculation using the same functional and basis set.

ASSOCIATED CONTENT

Supporting Information

The supporting information contains morphological study, along with the measurements of photoluminescence, EQE, TPV lifetimes and TD-DFT calculations

AUTHOR INFORMATION

Notes

The authors declare no competing financial interests.

ACKNOWLEDGMENT

JN acknowledges the Royal Society for a Wolfson Merit Award. JN, SMT and AAYG acknowledge the Engineering and Physical Sciences Research Council for support via grants EP/K029843/1, EP/K030671/1, EP/J017361/1. JY acknowledges support via an Imperial College Rector's Scholarship. MA acknowledges receipt of a Bourse d'Excellence from Ecole Polytechnique. TK acknowledges support from the DFG (Grant KI-1571/2-1). SMT acknowledges Hendrik Faber for AFM measurements.

REFERENCES

(1) Service, R. F. Outlook Brightens for Plastic Solar Cells. *Science* **2011** *332*, 293.

(2) Kaltenbrunner, M., White, M. S.; Glowacki; E. D., Sekitani, T.; Someya, T.; Saricifti, N. S.; Bauer, S. Ultratin and Lightweight Organic Solar Cells with High Flexibility *Nature Commun.* **2012**, *3*, 770.

(3) Chen, C., Chang, W., Yoshimura, K., Ohya, K., You, J., Gao, Yang, Y. An Efficient Triple-Junction Polymer Solar Cell Having a Power Conversion Efficiency Exceeding 11%. *Adv. Mater*. **2014**, *26*, 5670-5677.

(4) He, Z. C.; Xiao, B.; Liu, F.; Wu, H.; Yang, Y.; Xiao, S.; Wang, C.; Russel, T. P.; Cao, Y. Single-Junction Polymer Solar Cells With High Efficiency and Photovoltage. *Nature Photon*. **2015**, *9*, 174-179.

(5) Liu, Y.; Zhao, J.; Li, Z.; Mu, C.; Ma, W.; Hu, H.; Jiang, K.; Lin, H.; Ade, H. Aggregation and Morphology Control Enables Multiple Cases of High-Efficiency Polymer Solar Cells Nature Commun. **2014**, *5*, 5293.

(6) Vohra, V.; Kawashima, K.; Kakara, T.; Koganezawa, T.; Osaka, I.; Takimiya, K.; Murata, H. Efficient Inverted Polymer Solar Cells Employing Favourable Molecular Orientation. *Nature Photonics*. **2015**, *9*, 403–408.

(7) Zhang, Q, ; Kan, B.; Liu, F.; Long, G.; Wan, X.; Chen, X.; Yi Zuo, Ni, W.; Zhang, H.; Li, M.; Hu, Z.; Huang, F.; Cao, Y.; Liang, Z.; Zhang, M.; Russell, T. P.; Chen, Y. Small-molecule solar cells with efficiency over 9%. *Nature Photonics* **2015,** *9*, 35.

(8) Kan, B.; Qian Zhang, Q.; Li, M.; Wan, X; Ni, W.; Long, G.; Wang, Y.; Yang, X.; Feng, H.; Chen, Y. Solution-Processed Organic Solar Cells Based on Dialkylthiol-Substituted Benzodithiophene Unit with Efficiency near 10%. *J. Am. Chem. Soc.* **2014**, *136*, 15529-15532

(9) Liu, Y.; Chen, C.; Hong, Z.; Gao, J.; Yang, Y. (Michael); Zhou, H.; Dou, L.; Li, G.; Yang, Y. Solution-Processed Small-Molecule Solar Cells: Breaking The 10% Power Conversion Efficiency. *Sci. Rep.* **2013**, *3*, 3356.

(10) Sun, Y.; Welch. G. C.; Leong, W. L.; Takacs, C. J.; Bazan, G. C.; Heeger, A. J. Solution-Processed Small-Molecule Solar Cells with 6.7% Efficiency. *Nature Mater*. **2011,** *11*, 44-48.

(11) Mukherjee, S.; Proctor, C. M.; Tumbleston, J. R.; Bazan, G. C.; Nguyen, T.-Q.; Ade, H. Importance of Domain Purity and Molecular Packing in Efficient Solution-Processed Small-Molecule Solar Cells. *Adv. Mater*. **2015**, *27*, 1105–1111.

(12) Nayak, P. K.; Narasimhan, K. L.; Cahen, D. Separating Charges at Organic Interfaces: Effects of Disorder, Hot States, and Electric Field. *J. Phys. Chem. Lett.* **2013,** *4*, 1707-1717.

(13) Gao, K.; Li, L.; Lai, T.; Xiao, L.; Huang, Y.; Huang, F.; Peng, J.; Cao, Y.; Liu, F.; Russell, T. P.; Janssen, R. A. J.; Peng, X. Deep Absorbing Porphyrin Small Molecule for High-Performance Organic Solar Cells with Very Low Energy Losses. *J. Am. Chem. Soc.* **2015**, *137*, 7282-7285.

(14) Ran, N. A.; Kuik, M.; Love, J. A.; Proctor, C. M.; Nagao, I.; Bazan, G. C.; Nguyen, T.-Q. Understanding the Charge-Transfer State and Singlet Exciton Emission from Solution-Processed Small-Molecule Organic Solar Cells. *Adv. Mater.* **2014**, *26*, 7405–7412.

(15) Montcada, N. F. ; Domínguez, R. ; Pelado, B. ; Cruz, P. ; Palomares, E. ; Langa, F. High Photocurrent in Oligo-Thienylenevinylene-Based Small Molecule Solar Cells with 4.9% Solar-to-Electrical Energy Conversion. *J. Mater. Chem. A*, **2015**, *3*, 11340-11348.

(16) Yao, J.; Kirchartz, T.; Vezie, M. S.; Faist, M. A.; Gong, W.; He, Z.; Wu, H.; Troughton, J.; Watson, T.; Bryant D.; Nelson, J. Quantifying Losses in Open-Circuit Voltage in Solution-Processable Solar Cells. *Phys. Rev. Appl*., **2015**, *4*, 014020.

(17) Rau, U. Reciprocity Relation Between Photovoltaic Quantum Efficiency and Electroluminescent Emission of Solar Cells *Phys. Rev. B*, **2007**, *76*, 085303.

(18) Kirchartz, T.; Rau, U.; Kurth, M.; Mattheis, J.; Werner, J. H. Comparative Study of Electroluminescence from Cu(In,Ga)Se_2 and Si Solar Cells *Thin Solid Films* **2007**, *515*, 6238-6242.

(19) W. Shockley and H. J. Queisser. Detailed Balanced Limit of Efficiency of *p-n* Junction Solar Cells *J. Appl. Phys*. **1961**, *32*, 510-519.

(20) Koster, L.; Shaheen, S. E.; Hummelen, J. C. Pathways to a New Efficiency Regime for Organic Solar Cells *Adv. Energ. Mater*, **2012**, *2*, 1246-1253.

(21) Rau, U. Reciprocity Relation between Photovoltaic Quantum Efficiency and Electroluminescent Emission of Solar Cells. *Phys. Rev. B*, **2007**, *76*, 085303.

(22) Vandewal, K.; Albrecht, S.; Graham, K.R.; Widmer, J.; Douglas, J. D.; Schubert, M.; Mateker, W. R.; Bloking, J. T.; Burkhard, G. F.; Sellinger, A.; Fréchet, J. M. J.; Amassian, A.; Riede, M. K.; McGehee, M. D.; Neher, D.; Salleo, A. Efficient Charge Generation by Relaxed Charge-Transfer States at Organic Interfaces. *Nature Materials* **2013**, *13*, 63-68.

(23) Hörmann, U.; Kraus, J.; Gruber, M.; Schuhmair, C.; Linderl. T.; Grob, S.; Kapfinger, S.; Klein, K.; Stutzman, M.; Krenner, H. J.; Brütting, W. Quantification of Energy Losses in Organic Solar Cells from Temperature-Dependent Device Characteristics. *Phys. Rev. B* **2013**, *88*, 235307.

(24) Vandewal, K.; Widmer, J.; Brabec C, J.; Heumueller, T.; McGehee, M. D.; Leo K.; Riede, M.; Salleo, A. Increased Open-Circuit Voltage of Organic Solar Cells by Reduced Donor-Acceptor Interface Area'. *Adv. Mater.* **2014**, *26*, 3839-3843.

(25) Rau, U., Paetzold, U.W., Kirchartz, T. Thermodynamics of Light Management in Photovoltaic Devices *Phys. Rev. B,* **2014**, *90*, 035211.

(26) Bartynski, A. N.; Gruber, M.; Das, S.; Rangan, S.; Mollinger, S.; Trinh, C.; Bradforth, S. E.; Vandewal, K.; Salleo, A.; Bartynski, R. A.; Bruetting, W.; Thompson, M. E. Symmetry-Breaking Charge Transfer in a Zinc Chlorodipyrrin Acceptor for High Open Circuit Voltage Organic Photovoltaics *J. Am. Chem. Soc.* **2015**, *137*, 5397-5404.

(27) Tang, Z.; Liu, B.; Melianas, A.; Bergqvist, J.; Tress, W.; Bao, Q.; Qian, D.; Inganäs, O.; Zhang, F. A New Fullerene-Free Bulk-Heterojunction System for Efficient High-Voltage and High-Fill Factor Solution-Processed Organic Photovoltaics *Adv. Mater.* **2015**, *27*, 1900-1907.

(28) Li, Y.; Liu, X.; Wu, F.; Zhou, Y.; Jiang, Z.; Song, B.; Xia, Y.; Zhang, Z.; Gao, F.; Inganas, O.; Li, Y.; and Liao L. Non-fullerene acceptor with low energy loss and high external quantum efficiency: towards high performance polymer solar cells. *J. Mater. Chem. A*, **2016**, *4*, 5890.

(29) Baran, D.; Vezie, M. S.; Gasparini, N.; Deledalle, F.; Yao, J.; Schroeder, B. C.; Bronstein, H.; Ameri, T.; Kirchartz, T.; McCulloch, I.; Nelson, J.; Brabec, C. J. Role of Polymer Fractionation in Energetic Losses and Charge Carrier Lifetimes of Polymer: Fullerene Solar Cells. *J. Phys. Chem. C*, **2015**, *119*, 19668–19673.

(30) Few, S.; Frost, J. M.; Kirkpatrick, J.; Nelson, J. Influence of Chemical Structure on the Charge Transfer State Spectrum of a Polymer:Fullerene Complex , *J. Phys. Chem. C*, **2014**, *118*, 8253–8261.

(31) Veldman, D., Meskers, S. C. J.; Janssen, R. A. J. The Energy of Charge-Transfer States in Electron Donor-Acceptor Blends: Insight into the Energy Losses in Organic Solar Cells. *Adv. Funct. Mater.*, **2009**, *19*, 1939-1948.

(32) Frisch, M. J.; Trucks, G. W.; Schlegel, H. B.; Scuseria, G. E.; Robb, M. A.; Cheese-man, J. R.; Scalmani, G.; Barone, V.; Mennucci, B.; Petersson, G. A. *et al.* **Gaussian 09**, Revision A.1,.Gaussian, Inc., WallingfordCT, **2009**.

(33) Niedzialek, D.; Duchemin, I.; Branquinho de Queiroz, T.; Osella, S.; Rao, A.; Friend, R.; Blase, X.; Kümmel, S.; Beljonne, D. First Principles Calculations of Charge

Transfer Excitations in Polymer–Fullerene Complexes: Influence of Excess Energy. *Adv. Funct. Mater.* **2015**, *25*, 1972–1984.

(34) Faist, M. A.; Kirchartz, T.; Gong, W.; Ashraf, R. S.; McCulloch, I.; de Mello, J. C.; Ekins-Daukes, N. J.; Bradley, D. D. C.; Nelson, J. Competition Between the Charge Transfer State and the Singlet States of Donor or Acceptor Limiting the Efficiency in Polymer:Fullerene Solar Cells. *J. Am. Chem. Soc.* **2012**, *134*, 685−692.

(35) Vandewal, K.; Ma, Z.; Bergqvist, J.; Tang, Z.; Wang, E.; Henriksson, P.; Tvingstedt, K.; Andersson, M. R.; Zhang, F.; Inganäs, O. Quantification of Quantum Efficiency and Energy Losses in Low Bandgap Polymer:Fullerene Solar Cells with High Open-Circuit Voltage. *Adv. Funct. Mater.* **2012**, *22*, 3480–3490.

(36) Wang, E.; Zhang, Z.; Vandewal, K.; Henriksson, P.; Zhang, F.; Andersson, M. R.; Ma, Z.; Inganäs, O. An Easily Accessible Isoindigo- Based Polymer for High-Performance Polymer Solar Cells. *J. Am. Chem. Soc.*, **2011**, *133*, 14244−14247.

(37) Bijleveld, J. C.; Zoombelt, A. P.; Mathijssen, S.G. J.; Wienk, M. M.; Turbiez, M.; de Leeuw, D. M.; Rene A. J. Janssen, R. A. J. *J. Am. Chem. Soc*. **2009**, *131*, 16616–16617.